



# Numerical Investigation of Forced Convection of Nanofluid Flow in Microchannels: Effect of Adding Micromixer

A. Ababaei<sup>1</sup>, A. A. Abbasian Arani<sup>1</sup> and A. Aghaei<sup>2†</sup>

<sup>1</sup> *Department of Mechanical Engineering, University of Kashan, Kashan, Iran*  
<sup>2</sup> *Young Researchers and Elite Club, Arak Branch, Islamic Azad University, Arak, Iran*

†*Corresponding Author Email: alirezaaghaei21@gmail.com*

(Received November 6, 2016; accepted May 22, 2017)

## ABSTRACT

In the present study, forced convection of CuO–water nanofluid in a two dimensional parallel plate microchannel with and without micromixers has been investigated numerically. Two horizontal hot baffles were inserted between the adiabatic plates and three vertical baffles, which were attached on the plates, worked as micromixers in order to improve the cooling process. The effect of Reynolds number,  $Re = 10, 30, 60, 100,$  and  $150$  and nanoparticles volume fraction, from  $0$  to  $4\%$ , were examined on flow field and heat transfer. Different geometrical configurations for the arrangement of the hot baffles were tested. A FORTRAN code based on finite volume method was developed to solve the governing equations and SIMPLER algorithm was used for handling the pressure-velocity coupling. Simulations showed that the presence of micromixers and increasing the Reynolds number as well as nanoparticles volume fraction, increase the average Nusselt number. In order to achieve maximum heat transfer, best arrangements for the baffles were reported. It was also observed that the size of recirculation zones, which are created behind the micromixer baffles, increases with increasing Reynolds number and leads to better cooling.

**Keywords:** Forced convection; Microchannel; Micromixer arrangement; Koo-Kleinstreuer nanofluid model.

## NOMENCLATURE

$c_p$	specific heat capacity	$\nu$	kinematic viscosity
$d_{np}$	nanoparticles diameter	$\lambda, \xi$	empirical function
$k$	thermal conductivity	$\rho$	density
$L$	microchannel length	$\phi$	nanoparticles volume fraction
Nu	Nusselt number	<b>Subscripts</b>	
$p$	pressure	0	reference state value
$P$	dimensionless pressure	1, 2	baffle 1, baffle 2
Pr	Prandtl number	Avg	average
Re	Reynolds number	b	baffle
$T$	temperature	bf	base fluid
$(u, v)$	velocity components	Brownian	Brownian component of thermal conductivity
$(U, V)$	dimensionless velocity components	eff	effective
$(x, y)$	coordinates	h	hot baffle
$(X, Y)$	dimensionless coordinates	in	inlet flow
$\alpha$	thermal diffusivity	nf	nanofluid
$\delta x_i, \delta y_i$	baffle displacements	np	nanoparticles
$\theta$	dimensionless temperature	static	static component of thermal conductivity
$\kappa_B$	Boltzmann constant	<b>Superscripts</b>	
$\mu$	dynamic viscosity	*	dimensionless

## 1. INTRODUCTION

With the advent of nanofluids as a new type of fluids having ameliorated properties for heat transfer, copious researches have focused on the application of these fluids. Therefore, a plethora of experimental (Lomascolo *et al.* 2014; Malekzadeh *et al.* 2016) as well as numerical (Vanaki *et al.* 2015; Sheikholeslami and Ganji 2016; Raja *et al.* 2016) studies have been carried out in order to delve deeply into understanding the behavior of nanofluids. In recent years, Rahmati *et al.* (2016) employed a lattice Boltzmann method to simulate the mixed convection of Cu–water nanofluid in a double lid-driven cavity having sinusoidal temperature distribution. It was shown that at high Richardson numbers, the effect of changes of thermal phase deviation on the flow pattern is evident; while at low Richardson numbers the phase deviation changes do not affect the flow pattern. Aghaei *et al.* (2016) scrutinized the effect of magnetic field on mixed convection of Cu–water nanofluid in a trapezoidal enclosure. It was observed that with enforcing the magnetic field and intensifying it, both the nanofluid convection and the strength of the flow diminish and the flow tends towards natural convection and eventually towards pure conduction. In another study, Aghaei *et al.* (2016) investigated the mixed convection and entropy generation of CuO–water nanofluid inside a triangular enclosure for different inclination angles. It was observed that in all inclination angles both the average Nusselt number and entropy generation increase with volume fraction of nanoparticles. Battira and Bessaih (2016) conducted a numerical study on the natural convection of Al<sub>2</sub>O<sub>3</sub>–water in a vertical cylinder under radial and axial magnetic fields. The results indicated that for low values of Hartmann number ( $Ha \leq 20$ ) and at  $Ra=10^4$ , increasing the solid volume fraction decreases the heat transfer performance, especially if the magnetic field is applied axially. Mollamahdi *et al.* (2016) examined both the effect of chemical reaction and magnetic field in a channel with a permeable wall filled with Al<sub>2</sub>O<sub>3</sub>–Cu–water micropolar hybrid nanofluid. It was seen that when the hybrid nanofluid is utilized rather than pure nanofluid, the heat transfer coefficient will augment notably. Moreover, when the micropolar model is used, the Nusselt and Sherwood numbers are less than when it is not taken into account. Abbasian Arani *et al.* (2017) performed a numerical study simulating double-diffusive mixed convection of Al<sub>2</sub>O<sub>3</sub>–water inside a square enclosure considering various Richardson numbers, volume fraction of nanoparticles, and buoyancy ratios. Their results indicated that enhancing the volume fraction of nanoparticles reduces the average Nusselt number at high Richardson numbers, whereas at low Richardson numbers the opposite is true.

These studies have shown that nanofluids could be utilized in disparate applications in engineering, cooling of various devices, etc. A novel application of nanofluids could be found in modern medicine, for instance, where the nanodrugs are mixed in microchannels for controlled delivery with bio-

MEMS (Li, 2002). Such applications, like biological processing, lab on the chips, micro-reactors, and fuel cells, require rapid and complete mixing of fluid. Microchannel flows, due to very low flow rate, are characterized by very low Reynolds numbers. Owing to the predominantly laminar flow, it is difficult to achieve effective mixing fluids. If the mixing is obtained primarily by a diffusion mechanism, then fast mixing becomes impossible. Hence, microfluidic mixing is a very challenging problem because it requires fast and efficient mixing of low diffusivity fluids (Hsieh and Yang 2002). In general, micromixers are classified into two types: active and passive. In order to achieve rapid mixing in passive micromixers, obstacle structures were inserted into microchannels to enhance the advection effect via splitting, stretching, breaking and folding of liquid flows.

Chung *et al.* (2006) designed, fabricated and simulated a passive micromixer which contains some baffles with different arrangement. Alam and Kim (2012) numerically investigated the mixing of fluids in a microchannel with grooves in its side walls and found out that it has a better mixing performance than a smooth channel at  $Re > 10$ . Islami *et al.* (2013) numerically investigated the heat transfer of water–alumina nanofluid flow in microchannels containing micromixer. The results showed that the presence of micromixers increases heat transfer. It was also found that the main mechanism of enhancing heat transfer or mixing is the recirculation zones that are created behind the micromixers. The size of these zones increases with Reynolds number and baffle height.

In the past decades, forced and mixed convection of fluid flow through horizontal and vertical channels have been attracted much attention due to practical applications in electronic devices, heat exchangers, nuclear reactors, and lots of different thermal systems. Many researchers have investigated various boundary conditions on heat transfer inside the channels. Symmetrical and asymmetrical heating with constant temperature or heat flux are investigated analytically (Yao 1983; Fourcher and Mansouri 1998; Nield 2004), numerically (Jenn-Wuu *et al.* 1976; Vijayan and Balaji 2004; Guimarães and Menon 2008), and experimentally (Hatay *et al.* 1991; Hwang *et al.* 1992; Kurtbas and Celik 2009). Barletta *et al.* (2005) numerically studied the mixed convection flows in a vertical channel.

Effect of Prandtl and Reynolds numbers on the fluid flow and heat transfer have also been investigated. Elpidorou *et al.* (1991) reported the results of numerical simulations of forced and mixed convection in a vertical channel. In these simulations, a heat source with constant heat flux was inserted on one of the vertical walls while the other walls were adiabatic or with constant temperature. For various boundary conditions, effect of Grashof and Reynolds numbers were examined on the fluid flow and heat transfer rate. The results demonstrated that the size of the convective cells is intensely related to Grashof and Reynolds numbers. Mahaney *et al.* (1990), both

experimentally and numerically, investigated the mixed convection heat transfer from an array of discrete sources in a horizontal rectangular channel. The results illustrated that the heat transfer enhances as the Rayleigh number increases.

Furthermore, many researchers have investigated the convective heat transfer inside channels and microchannels with fins. In a numerical study, air flow and heat transfer characteristics in entrance region of a horizontal channel with transverse fins were investigated by Bazdidi-Tehrani and Naderi-Abadi (2004). The results showed that the Nusselt number increases but the friction decreases as the pitch of the fins increases. Alamyane and Mohamad (2010) numerically investigated the forced convection in a channel with extended surfaces placed on the lower hot wall. In more recent years, Kaya (2016) used a Fluent CFD code to analyze the effect of ramification length and angle on pressure drop as well as heat transfer in a ramified microchannel and compared the results with the analytical existing ones. The results showed a good agreement with the mathematical model and also demonstrated that the pressure drop increases with increasing both the ramification length and angle. Moreover, the maximum temperature inside the ramified microchannel increases with increasing the ramification length or the ratio volume fraction of ethanol. Malvandi and Ganji (2016) theoretically investigated the effect of nanoparticle migration via Brownian motion and the thermophoresis on mixed convection of water–alumina nanofluid in a vertical microchannel considering slip condition in the presence of heat source/sink. The simulations demonstrated that the buoyancy effect due to the temperature distribution is insignificant; however, the buoyancy effect due to the concentration distribution of nanoparticles has considerable impact on the flow and heat transfer characteristics. Ababaei and Abbaszadeh (2017) analyzed entropy generation in forced convective slip flow of nanofluid inside a microchannel with square impediments at low Reynolds numbers. The effect of Reynolds and Knudsen numbers and volume fraction of nanoparticles were examined. It was seen that by increasing the Knudsen number both the total entropy generation rate and average Nusselt number decrease. Abbaszadeh *et al.* (2017) investigated the effect of magnetic field on forced convection and entropy generation of CuO–water nanofluid in a parallel plate microchannel considering slip velocity and temperature jump. The results show that when the Hartmann or Reynolds numbers, or the volume fraction of nanoparticles increase, the average Nusselt number and the total entropy generation rate increase. Furthermore, when Knudsen number increases, the total entropy generation rate decreases.

Based on the aforementioned studies, forced convection of nanofluids in a microchannel containing micromixers has gained little attention. The purpose of this study is to examine the effect of adding the micromixers, as well as Reynolds number and nanoparticles volume fraction in different geometrical arrangements for the hot baffles, on the nanofluid flow field and heat transfer characteristics.

## 2. GOVERNING EQUATIONS AND BOUNDARY CONDITIONS

A schematic view of the physical problem and boundary conditions is shown in Fig. 1. The steady, laminar inlet flow is hydrodynamically fully developed with uniform temperature. The two plates of the microchannel are adiabatic and there is no slip velocity or temperature jump between the nanofluid and the plates. At the outlet port temperature and velocity gradients are set to zero. Length of the microchannel is 8 times its height (except for  $Re = 100, 150$  with micromixers where length is 13 and 20 times its height, respectively) and three micromixers are placed at  $X = 0.5L, 2L, 3.5L$  and two hot baffles are placed at  $(X_1, Y_1) = (1.25 + \delta x_1, 0.5 + \delta y_1)L$  and  $(X_2, Y_2) = (2.75 + \delta x_2, 0.5 + \delta y_2)L$ . Height of the micromixers is  $0.5L$  and lengths of the hot baffles are  $L_i = (0.5 \pm 0.25)L$ .

The thermophysical properties of water and CuO are mentioned in Table 1. Variable properties of nanofluid are approximated by the Koo and Kleinstreuer (2004) nanofluid model.

The dimensionless variable properties form of the governing equations for laminar, steady, two-dimensional forced convection of nanofluid is given as:

$$\frac{\partial}{\partial X}(\rho^*U) + \frac{\partial}{\partial Y}(\rho^*V) = 0 \tag{1}$$

$$\frac{\partial}{\partial X}(\rho^*UU) + \frac{\partial}{\partial Y}(\rho^*UV) = -\frac{\partial P}{\partial X} + \frac{1}{Re} \left( \frac{\partial}{\partial X} \left( \mu^* \frac{\partial U}{\partial X} \right) + \frac{\partial}{\partial Y} \left( \mu^* \frac{\partial U}{\partial Y} \right) \right) \tag{2}$$

$$\frac{\partial}{\partial X}(\rho^*VU) + \frac{\partial}{\partial Y}(\rho^*VV) = -\frac{\partial P}{\partial Y} + \frac{1}{Re} \left( \frac{\partial}{\partial X} \left( \mu^* \frac{\partial U}{\partial X} \right) + \frac{\partial}{\partial Y} \left( \mu^* \frac{\partial U}{\partial Y} \right) \right) \tag{3}$$

$$\frac{\partial}{\partial X}(\rho^*c_p^*U\theta) + \frac{\partial}{\partial Y}(\rho^*c_p^*V\theta) = \frac{1}{RePr} \left( \frac{\partial}{\partial X} \left( k^* \frac{\partial U}{\partial X} \right) + \frac{\partial}{\partial Y} \left( k^* \frac{\partial U}{\partial Y} \right) \right) \tag{4}$$

The following dimensionless variables are used to nondimensionalize the governing equations:

$$\begin{aligned} (X, Y) &= \frac{(x, y)}{L}; (U, V) = \frac{(u, v)}{u_{in}} \\ \theta &= \frac{T - T_{in}}{T_h - T_{in}}; P = \frac{p}{\rho_{bf} u_{in}^2}; \rho^* = \frac{\rho_{nf}}{\rho_{bf,0}} \\ c_p^* &= \frac{(c_p)_{nf}}{(c_p)_{bf,0}}; \mu^* = \frac{\mu_{nf}}{\mu_{bf,0}}; k^* = \frac{k_{nf}}{k_{bf,0}} \\ Re &= \frac{u_{in} L}{\nu_{bf}}; Pr = \frac{\nu_{bf}}{\alpha_{bf}} \end{aligned} \tag{5}$$

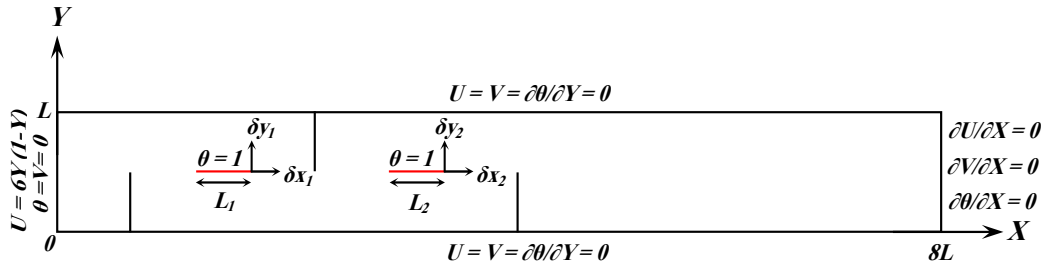


Fig. 1. Geometrical configuration and boundary conditions.

Table 1 Thermophysical properties of the base fluid and the nanoparticles (Mahian *et al.* 2012)

	$\rho$ (kg m <sup>-3</sup> )	$c_p$ (J kg <sup>-1</sup> K <sup>-1</sup> )	$K$ (W m <sup>-1</sup> K <sup>-1</sup> )	$\beta$ (K <sup>-1</sup> )
Water	997.1	0.613	4179	$2.1 \times 10^{-4}$
CuO	6320	76.5	535.6	$1.8 \times 10^{-4}$

In Eqs. (1)-(4) the nanofluid effective density and specific heat capacitance are given as:

$$\rho_{nf} = (1 - \phi)\rho_{bf} + \phi\rho_{np} \quad (6)$$

$$(\rho c_p)_{nf} = (1 - \phi)(\rho c_p)_{bf} + \phi(\rho c_p)_{np} \quad (7)$$

The effective dynamic viscosity and thermal conductivity of nanofluid are approximated by the Koo and Kleinstreuer (2004) model as:

$$\mu_{eff} = \mu_{static} + \mu_{Brownian} \quad (8)$$

$$k_{eff} = k_{static} + k_{Brownian} \quad (9)$$

where the static viscosity and the static thermal conductivity are approximated by the Brinkman (1952) and Maxwell-Garnett (1904) correlations, respectively:

$$\mu_{static} = \mu_{bf}(1 - \phi)^{-2.5} \quad (10)$$

$$k_{static} = k_{bf} \frac{(k_{np} + 2k_{bf}) - 2\phi(k_{bf} - k_{np})}{(k_{np} + 2k_{bf}) + \phi(k_{bf} - k_{np})} \quad (11)$$

and the Brownian components of the effective dynamic viscosity and thermal conductivity are given by:

$$\mu_{Brownian} = 5 \times 10^4 \lambda \phi \rho_{bf} \sqrt{\frac{\kappa_B T}{\rho_{np} d_{np}}} \xi(T, \phi) \quad (12)$$

$$k_{Brownian} = 5 \times 10^4 \lambda \phi \rho_{bf} c_{p, bf} \sqrt{\frac{\kappa_B T}{\rho_{np} d_{np}}} \xi(T, \phi) \quad (13)$$

where  $\rho_{np}$  and  $d_{np}$  are the density and the diameter of nanoparticles ( $d_{np} = 29$  nm), respectively. For CuO–water nanofluid  $\lambda$  and  $\xi$  are two empirical functions that are given by:

$$\lambda = 0.0137(100\phi)^{-0.8229} \quad \phi \leq 1\% \quad (14)$$

$$\lambda = 0.0011(100\phi)^{-0.7272} \quad \phi > 1\%$$

$$\xi(T, \phi) = (-6.04\phi + 0.4705)T + (1722.3\phi - 134.63) \quad (15)$$

$$1\% \leq \phi \leq 4\%; \quad 300 \leq T \text{ (K)} \leq 325$$

The local Nusselt number on each baffle surface can be written as:

$$Nu = -\frac{k_{nf}}{k_{bf}} \frac{\partial \theta}{\partial Y} \Big|_{Y=Y_b} \quad (16)$$

The average Nusselt number on baffles is determined from:

$$Nu_{Avg} = \frac{1}{L_1 + L_2} \left( \int_{L_1} Nu dX + \int_{L_2} Nu dX \right) \quad (17)$$

### 3. NUMERICAL SIMULATION

The governing equations are solved using finite volume method and SIMPLER algorithm is used for handling the pressure-velocity coupling. The diffusion terms in the governing equations are discretized using second-order central difference scheme, and to discretize the convective terms hybrid scheme is employed. The line-by-line TDMA method is applied on the equation systems until relative residuals became less than  $10^{-7}$ . To obtain converged solutions, under-relaxation factors 0.5 and 0.7 are used for the momentum and energy equations, respectively.

#### 3.1 Grid Independence Study

A uniform staggered grid system is used for discretizing the governing equations. In order to find an independent grid system, the average Nusselt number on hot baffles with micromixers is obtained for different grid systems and reported in Table 2. From this table, the average Nusselt numbers show that a grid system of  $568 \times 71$  is suitable for computations.

#### 3.2 Code Validation

In order to validate the present code, two numerical studies were simulated and the results obtained

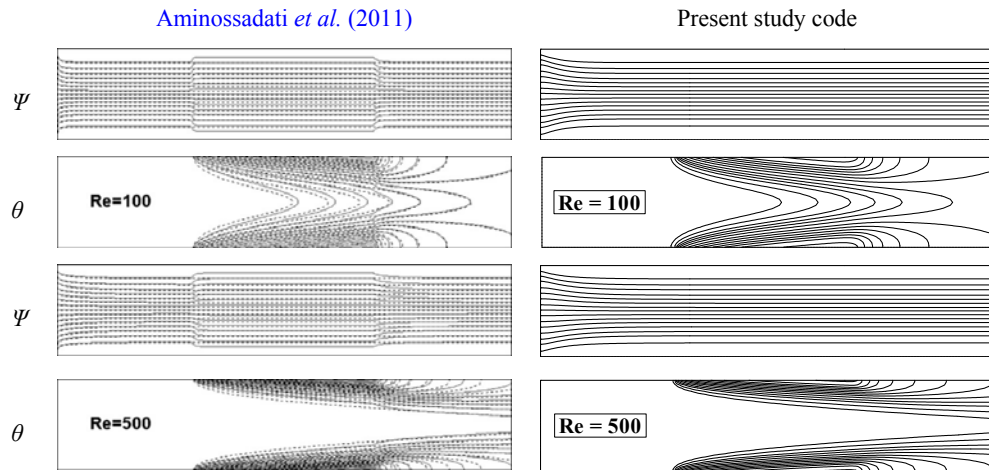


**Fig. 2. Comparison between the results obtained by present study code and Aminossadati *et al.* (2011) with uniform heat flux in central part at Re = 100 and 500, Pr = 6.2, and Ha = 0 for Al<sub>2</sub>O<sub>3</sub>-water nanofluid with  $\phi = 2\%$ .**

from the present code were compared with the existing results of those studies. In the first case, the average Nusselt numbers acquired from the present code for the problem of mixed convection in a lid-driven triangular enclosure filled with nanofluids are compared with those of Ghasemi and Aminossadati (2010) in Table 3. In the second case, the problem of forced convection of nanofluid in a partially heated microchannel in the presence of magnetic field is simulated with the present study code and the results were compared with the results of Aminossadati *et al.* (2011) in Fig. 2. Comparison between the results of these studies with the present code simulations shows an insignificant difference and ensures proper simulation via the present code.

**Table 2 Average Nusselt number for Re = 30 and  $\phi = 0.02$**

Grid size	408×51	488×61	568×71	648×81
Nu <sub>Avg</sub>	16.07	16.35	16.50	16.51

**Table 3 Average Nusselt number obtained from the present code compared with those of Ghasemi and Aminossadati (2010)**

Ri	$\phi$ (%)	Present study code	Ghasemi and Aminossadati (2010)	Difference (%)
0.1	1	30.158	30.326	0.55
	3	31.964	32.274	0.96
10	1	11.211	11.463	2.20
	3	11.896	12.258	2.95

## 4. RESULTS AND DISCUSSION

### 4.1 Effect of Adding the Micromixers

In this section, the numerical results of fluid flow and heat transfer characteristics for both with and without micromixer cases are reported and compared. Streamlines and isotherm contours at different Reynolds numbers are presented and average Nusselt numbers for both cases are compared.

Streamlines and isotherms for a fixed nanoparticles volume fraction of 0.02 at different Reynolds numbers without the micromixers are shown in Fig. 3. Before and after the hot baffles, streamlines show insignificant difference at various Reynolds numbers and they are mostly parallel. On the hot baffles a little deviation is observed due to existence of the baffles, and increasing the Reynolds number results in reducing the deviation. This happens because of the increase of inertial forces due to higher Reynolds numbers. According to isotherm contours of Fig. 3, flow temperature increases as the flow reaches the first hot baffle. Increasing the Reynolds number makes the isotherms more compressed, which increases the temperature gradient across the microchannel as well as heat transfer. At higher Reynolds numbers, isotherms have more inclination to reach the end of the microchannel. This behavior is seen especially for isotherms with lower temperature at the beginning of the microchannel. At high Reynolds numbers, cold nanofluid flow of the inlet port, near the top and bottom walls of the microchannel, continues to reach the outlet port, while at Re = 10 after the second hot baffle the nanofluid flow is not cold.

Figure 4 shows streamlines and isotherms for  $\phi=0.02$  with micromixers at different Reynolds numbers. Three micromixers are placed before the

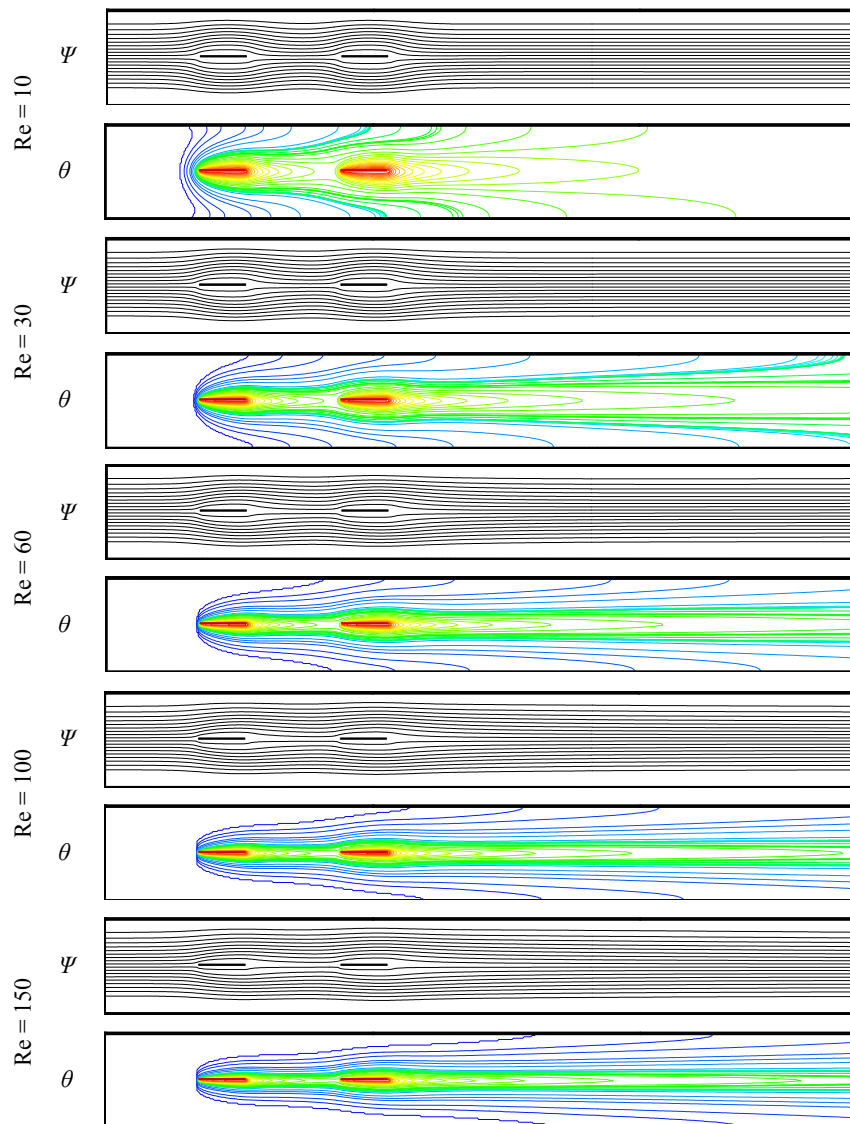


**Fig. 3. Streamlines and isotherms at different Reynolds numbers for  $\phi = 0.02$  without the micromixer.**

first hot baffle, between the two hot baffles and after the second hot baffle. Streamlines of the Fig. 4 show that vortexes are formed after each micromixer and increasing Reynolds number makes the vortexes larger. At  $Re = 60$ , there is a small vortex right before the third micromixer and the biggest vortex forms after the third micromixer for all Reynolds numbers. At higher Reynolds numbers more vortexes are formed. Compared to the case of no micromixers, adding the micromixers makes the streamlines and isotherms more curved and compressed, which leads to heat transfer increase.

By adding the micromixers, the cold nanofluid flow, near the top and bottom walls of the microchannel, is brought to the middle of the microchannel, which also increases the heat transfer. Analogous to no micromixer case, isotherms tend to reach the end of the microchannel as the Reynolds number increases.

Figure 5 shows the effect of nanoparticles volume fraction on the average Nusselt number at different Reynolds numbers for both cases of with and without the micromixers. For all Reynolds numbers, the average Nusselt number increases with increasing the nanoparticles volume fraction for both cases of with and without micromixers. The thermal conductivity of nanofluid increases when the nanoparticles volume fraction increases, which causes an increase in heat transfer as well as average Nusselt number.

In Fig. 5 by comparing the average Nusselt numbers of the both cases, it is observed that adding the micromixers enhances the average Nusselt number. Adding the micromixers makes the streamlines more curved, which leads to better displacement of nanofluid and enhanced convective heat transfer. After the micromixers, some vortexes are formed, which have a significant role in

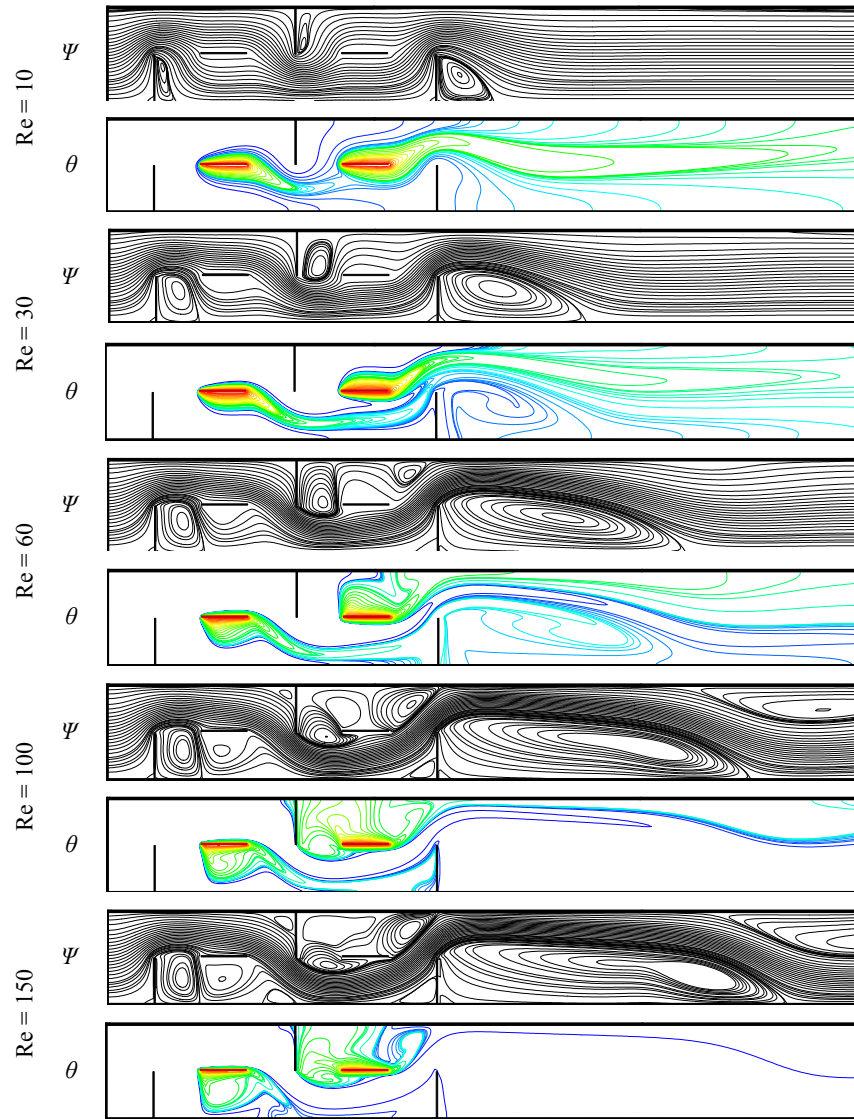
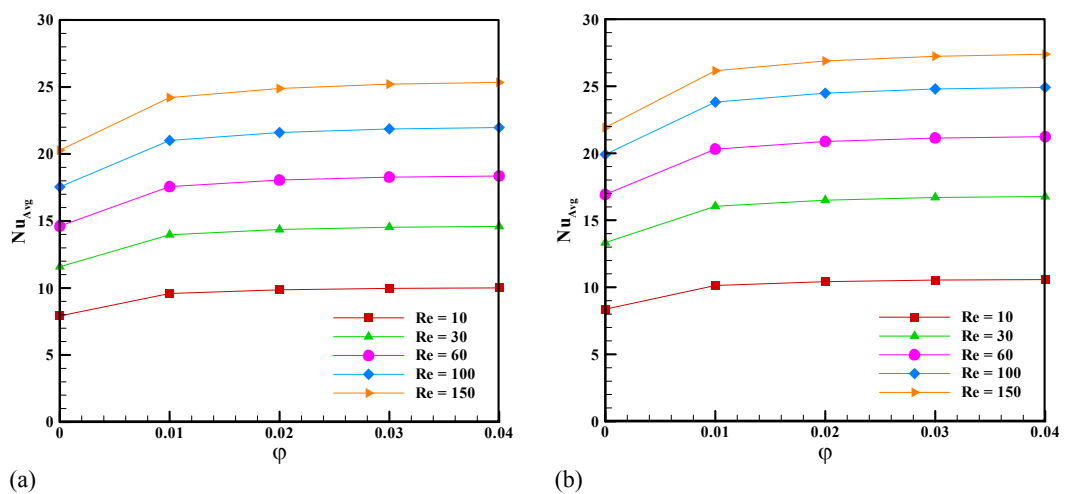


Fig. 4. Streamlines and isotherms at different Reynolds numbers for  $\phi = 0.02$  with the micromixers.



(a) (b)  
Fig. 5. Effect of nanoparticles volume fraction on the average Nusselt number at different Reynolds numbers: (a) without the micromixers (b) with the micromixers.

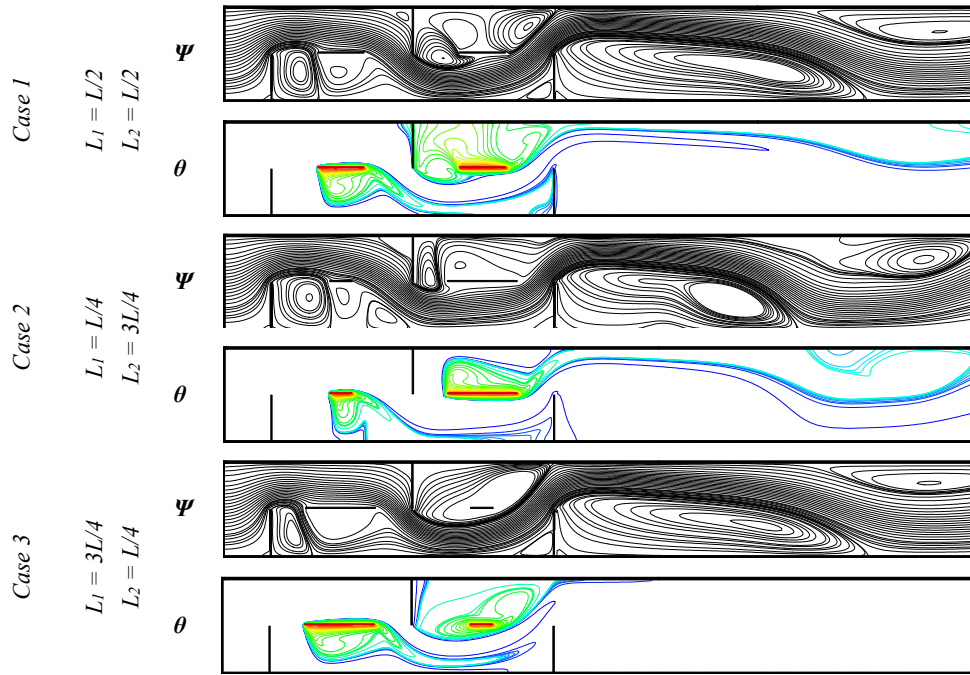


Fig. 6. Streamlines and isotherms for different size of hot baffles at  $Re = 100$  and  $\phi = 0.02$ .

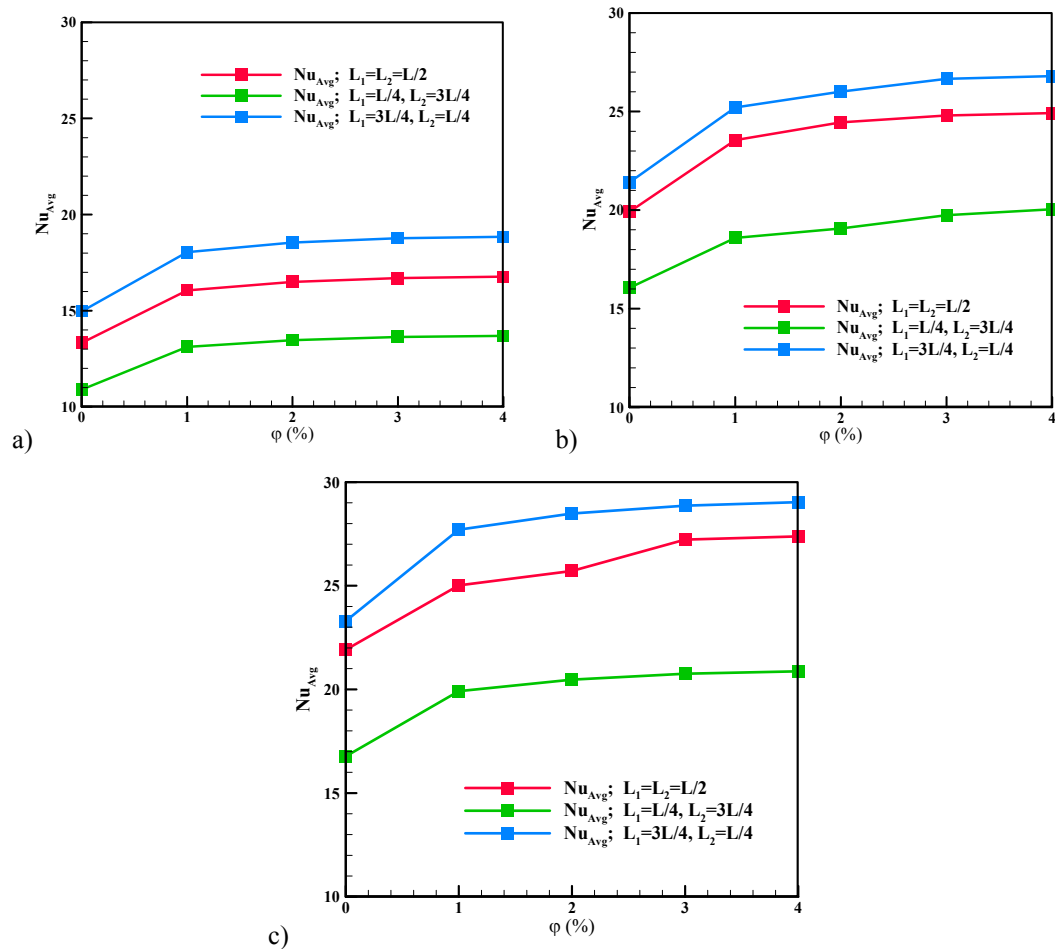
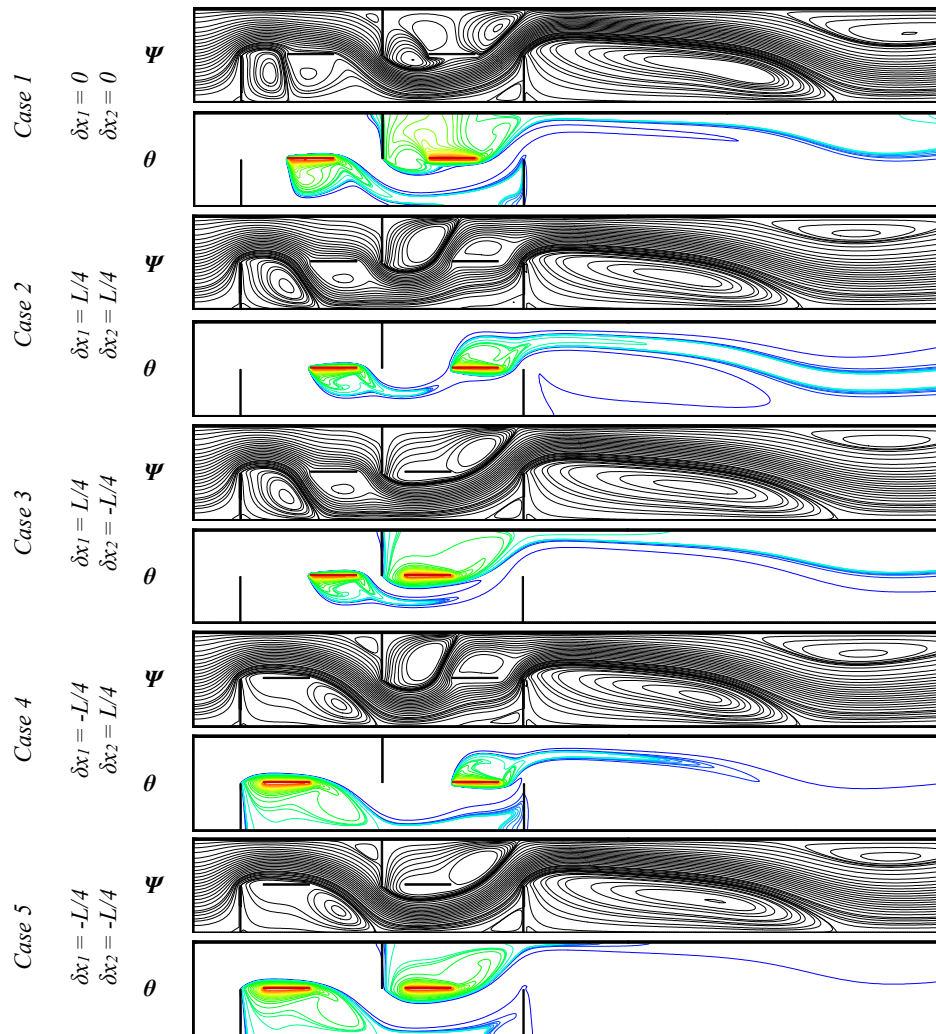


Fig. 7. Effects of size of hot baffles on the average Nusselt number for different nanoparticles volume fraction at: (a)  $Re = 30$  (b)  $Re = 100$  (c)  $Re = 150$ .



**Fig. 8.** Streamlines and isotherms for different horizontal arrangements at  $Re = 100$  and  $\phi = 0.02$ .

augmenting the heat transfer. By adding the micromixers the maximum and minimum enhancement of the average Nusselt numbers are 15.78% and 3.31%, respectively for  $\phi = 0$  at  $Re = 60$ , and for  $\phi = 0.02$  at  $Re = 150$ .

#### 4.2 Effect of the size of hot baffles

In this section, three arrangements for the size of hot baffles are considered. Streamlines and isotherms for these cases are shown in Fig. 6 at  $Re=100$  and  $\phi = 0.02$ . By comparing streamlines of the first and the second case, when the length of the second hot baffle increases, the flow becomes more compressed over the third micromixer and the vortexes over this baffle become smaller. In the third case, when the first hot baffle is large, least number of vortexes is seen over or under the baffles. Compared to the first case, the isotherms have an enhanced tendency to reach the end of the microchannel and the temperature gradient is lower in the second case, while in the third case, the flow after the third micromixer is entirely cold and the temperature gradient and heat transfer is higher.

Effects of size of the hot baffles on the average

Nusselt number can be seen in Fig. 7. The average Nusselt number on hot baffles is shown for different nanoparticles volume fractions at different Reynolds numbers. Increasing Reynolds number or nanoparticles volume fraction results in an increase in the average Nusselt number. Average Nusselt number on smaller hot baffles is always higher than the large ones. It happens due to fact that smaller impediment leads to better movement of the nanofluid flow and more temperature gradient. Maximum heat transfer occurs in the third case where the second baffle is smaller and has a relatively large average Nusselt number which significantly affects the overall average Nusselt number. The minimum overall average Nusselt number occurs in the second case where the first hot baffle is smaller. So, the second case has the worst arrangement of the baffles.

#### 4.3 Effect of Horizontal Place of Hot Baffles

Five arrangements for the horizontal place of hot baffles are considered in this section. In Fig. 8 the streamlines and isotherms for these cases are shown

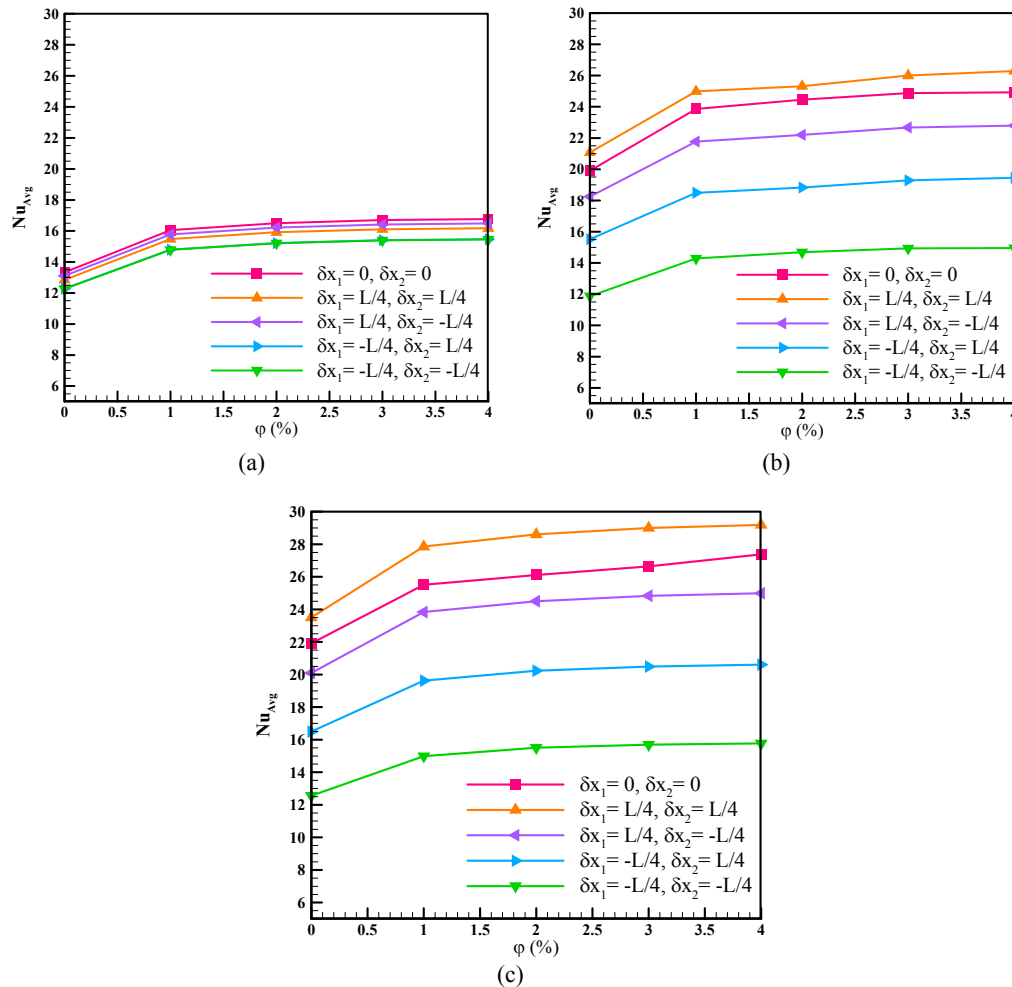


**Fig. 9.** Effects of horizontal place of hot baffles on the average Nusselt number for different nanoparticles volume fraction at: (a)  $Re = 30$  (b)  $Re = 100$  (c)  $Re = 150$ .

at  $Re = 100$  and  $\phi = 0.02$ . In the first case where the baffles are in the middle of two micromixers, many secondary vortices are formed. In all of the other cases some of these vortices vanish. When each baffle is placed in the forward position, the nanofluid flow separates and flows both over and under the baffles. In the backward position, the baffles have a little influence on the nanofluid flow and the flow passes easily besides the baffles. By comparing the isotherms, when each baffle is placed in the forward position, the isotherms are more compressed and the temperature gradient and heat transfer is higher in those cases.

Effect of horizontal place of hot baffles at different Reynolds numbers and for different nanoparticles volume fractions on the overall average Nusselt number is shown in Fig. 9. At  $Re = 30$  maximum Nusselt number is for the first case where the baffles are in the middle position. It should be noted that the average Nusselt number for the fourth and fifth cases are almost identical. At high Reynolds numbers ( $Re = 100, 150$ ) the average Nusselt number of the second case is more than that of the first case. It happens due to separation of the flow

because of the baffles placed in the forward position, which makes the nanofluid flow both over and under the baffles and helps cooling from both sides. The minimum average Nusselt number is always for the fifth case which has the worst arrangement of the baffles.

#### 4.4 Effect of vertical place of hot baffles

In this section, five other arrangements are considered for the vertical place of hot baffles. The streamlines and isotherms of these cases are shown in Fig. 10 at  $Re = 100$  and  $\phi = 0.02$ . When the first baffle is placed in the upper position (or the second one in the lower position), the flow completely passes from both sides of this baffle. But when it is placed in the lower position, the flow passes over the baffle and a vortex encircles it. The most compressed isotherms are for the third case where the flow passes over and under the two baffles. The worst arrangement is for the fourth case where the flow has a little contact with the surfaces of two baffles.

Effect of vertical place of hot baffles is shown in Fig. 11. Minimum average Nusselt number is

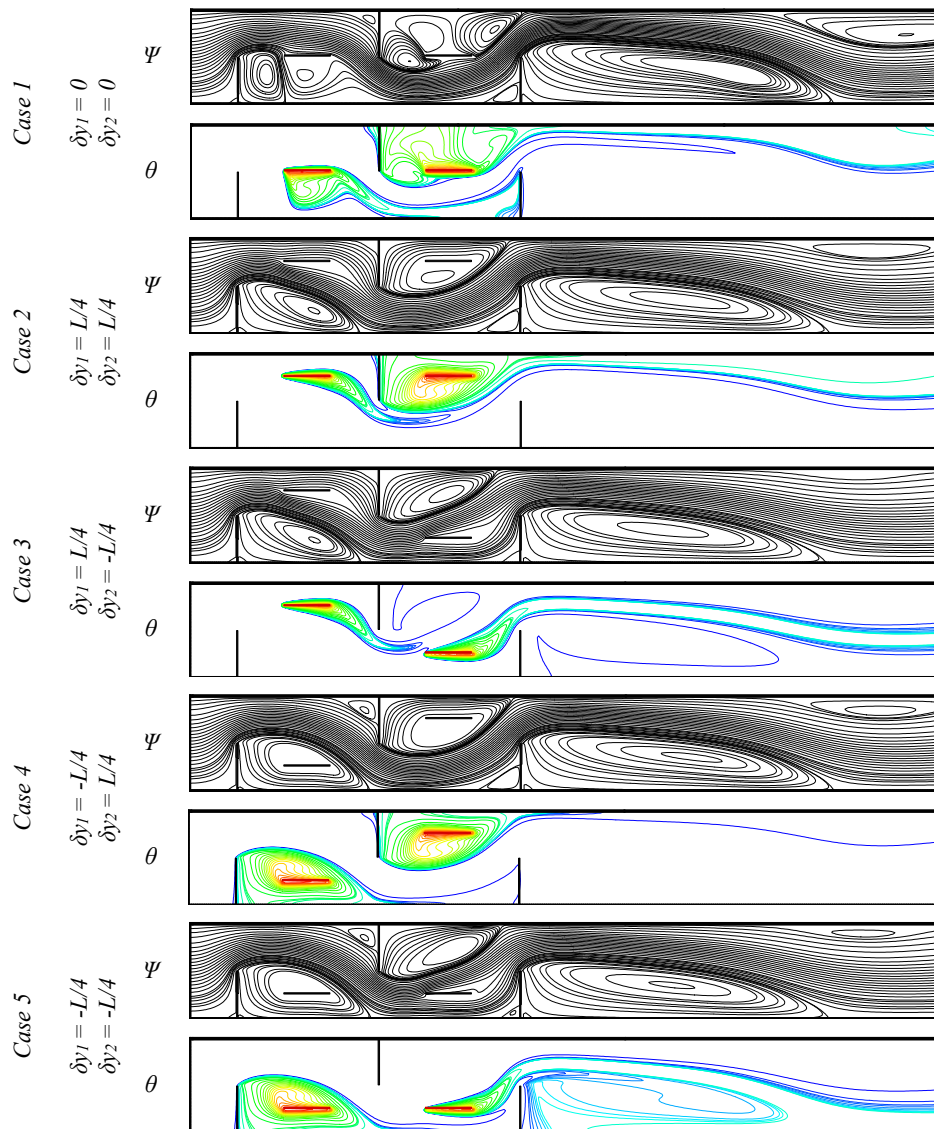


**Fig. 10.** Streamlines and isotherms for different vertical arrangements at  $Re = 100$  and  $\phi = 0.02$ .

always for the fourth case as it was mentioned earlier. First case of the arrangements has the maximum Nusselt number at  $Re = 30$ , but at higher Reynolds numbers, the third case has the maximum Nusselt number. This is due to the flow separation in this case where the two baffles force the flow to pass from both sides of them.

## 5. CONCLUSION

In this study forced convection of CuO–water nanofluid in a two dimensional parallel plate microchannel with and without micromixers was investigated numerically. The effect of independent parameters such as Reynolds number ranging from 10 to 150 and nanoparticles volume fraction ranging from 0 to 0.04 were studied on the flow field and heat transfer. Some geometrical configurations for the arrangement of the baffles were examined.

The following conclusions were drawn from this

study:

1. For the case of no micromixers, the isotherms compress with increasing the Reynolds number which indicates enhancement of heat transfer. Increasing the Reynolds number also causes more inclination in isotherms to reach the end of the microchannel.
2. For both cases of with and without the micromixers, average Nusselt numbers increase with increasing the nanoparticles volume fraction of at all Reynolds numbers.
3. In the presence of micromixers, increasing the Reynolds number leads to larger vortices behind the micromixers. The maximum and minimum enhancement of the average Nusselt numbers after adding the micromixers are 15.78% and 3.31%, respectively for  $\phi = 0$  at  $Re = 60$  and for  $\phi = 0.02$  at  $Re = 150$ .

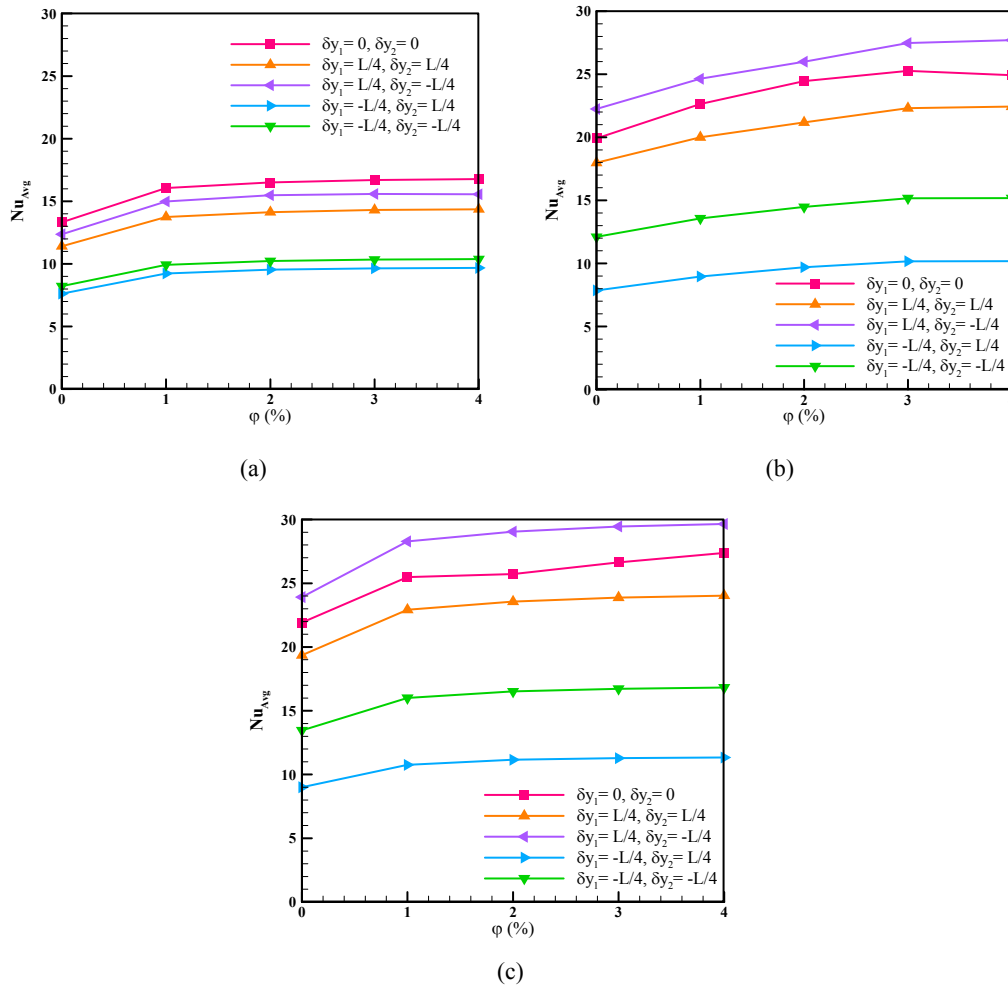


**Fig. 11. Effects of vertical place of hot baffles on the average Nusselt number for different nanoparticles volume fraction at: (a) Re = 30 (b) Re = 100 (c) Re = 150.**

4. Considering different arrangements for the size of hot baffles, maximum heat transfer occurs where the second baffle is smaller. The minimum overall average Nusselt number occurs where the first hot baffle is smaller.
5. Considering different arrangements for the horizontal place of hot baffles, at high Reynolds numbers the best arrangement is the one where the two baffles are placed in forward position which makes the nanofluid flows both over and under the baffles and helps the cooling from both sides. The worst arrangement is always where the two baffles are placed in backward position.
6. Considering different arrangements for the vertical place of hot baffles, the worst arrangement is always where the two baffles are placed behind the micromixers. In this case the baffles have a little contact with the main stream of nanofluid which worsens the heat transfer. At high Reynolds numbers the best arrangement is where the first baffle is placed in upper position and the second one is placed in lower position. In this case the nanofluid

flows both over and under the baffles.

#### ACKNOWLEDGEMENTS

The authors are profoundly grateful to the Division of Research Affairs of University of Kashan for supporting this study (Grant No. 55806).

#### REFERENCES

Ababaei, A. and M. Abbaszadeh (2017). Second Law Analyses of Forced Convection of Low-Reynolds-Number Slip Flow of Nanofluid Inside a Microchannel with Square Impediments. *Global Journal of Nanomedicine* 1(4).

Abbasian Arani, A. A., A. Ababaei, G. A. Sheikhzadeh and A. Aghaei (2017). Numerical simulation of double-diffusive mixed convection in an enclosure filled with nanofluid using Bejan's heatlines and masslines. *Alexandria Engineering Journal*.

Abbaszadeh, M., A. Ababaei, A. A. Arani and A.

- A. Sharifabadi (2017). MHD forced convection and entropy generation of CuO-water nanofluid in a microchannel considering slip velocity and temperature jump. *Journal of the Brazilian Society of Mechanical Sciences and Engineering* 39,775-790.
- Aghaei, A., H. Khorasanizadeh, G. Sheikhzadeh and M. Abbaszadeh (2016). Numerical study of magnetic field on mixed convection and entropy generation of nanofluid in a trapezoidal enclosure. *Journal of Magnetism and Magnetic Materials* 403, 133-145.
- Alam, A., and K. Y. Kim (2012). Analysis of mixing in a curved microchannel with rectangular grooves. *Chemical Engineering Journal* 181, 708-716.
- Alamyane, A. A. and A. A. Mohamad (2010). Simulation of forced convection in a channel with extended surfaces by the lattice Boltzmann method. *Computers & Mathematics with Applications* 59(7), 2421-2430.
- Aminossadati, S. M., A. Raisi and B. Ghasemi (2011). Effects of magnetic field on nanofluid forced convection in a partially heated microchannel. *International Journal of Non-Linear Mechanics* 46(10), 1373-1382.
- Barletta, A., E. Magyari and B. Keller (2005). Dual mixed convection flows in a vertical channel. *International Journal of Heat and Mass Transfer* 48(23), 4835-4845.
- Brinkman, H. C. (1952). The viscosity of concentrated suspensions and solutions. *The Journal of Chemical Physics*, 20(4), 571-571.
- Chung, C. K., C. Y. Wu, T. R. Shih, C. F. Wu and B. H. Wu (2006). Design and Simulation of a Novel Micro-mixer with Baffles and Side-wall Injection into the Main Channel. In *2006 1st IEEE International Conference on Nano/Micro Engineered and Molecular Systems* 721-724 IEEE.
- Elpidorou, D., V. Prasad and V. Modi (1991). Convection in a vertical channel with a finite wall heat source. *International journal of heat and mass transfer* 34(2), 573-578.
- Fourcher, B. and K. Mansouri (1998). Theoretical study of periodic turbulent forced convection inside a parallel-plate channel. *International journal of engineering science* 36(4), 411-420.
- Ghasemi, B. and S. M. Aminossadati (2010). Mixed convection in a lid-driven triangular enclosure filled with nanofluids. *International Communications in Heat and Mass Transfer* 37(8), 1142-1148.
- Guimarães, P. M. and G. J. Menon (2008). Combined free and forced convection in an inclined channel with discrete heat sources. *International Communications in Heat and Mass Transfer* 35(10), 1267-1274.
- Hatay, F. F., W. Li, S. Kakaç and F. Mayinger (1991). Numerical and experimental analysis of unsteady laminar forced convection in channels. *International communications in heat and mass transfer* 18(4), 407-417.
- Hsieh, C. Y. and A. S. Yang (2009). Mixing enhancement of a passive micromixer by applying boundary protrusion structures. In *Advanced Materials Research* 74, 77-80. Trans Tech Publications.
- Hwang, T. H., Y. Cai and P. Cheng (1992). An experimental study of forced convection in a packed channel with asymmetric heating. *International journal of heat and mass transfer* 35(11), 3029-3039.
- Islami, S. B., B. Dastvareh and R. Gharraei (2013). Numerical study of hydrodynamic and heat transfer of nanofluid flow in microchannels containing micromixer. *International Communications in Heat and Mass Transfer* 43, 146-154.
- Jenn-Wuu, O., K. C. Cheng and L. Ran-Chau (1976). Combined free and forced laminar convection in inclined rectangular channels. *International Journal of Heat and Mass Transfer* 19(3), 277-283.
- Koo, J., and C. Kleinstreuer (2004). A new thermal conductivity model for nanofluids. *Journal of Nanoparticle Research* 6(6), 577-588.
- Kurtbas, I., and N. Celik (2009). Experimental investigation of forced and mixed convection heat transfer in a foam-filled horizontal rectangular channel. *International Journal of Heat and Mass Transfer* 52(5), 1313-1325.
- Li, J. (2008). *Computational Analysis of Nanofluid Flow in Microchannels with Applications to Micro-heat Sinks and Bio-MEMS*. ProQuest.
- Lomascolo, M., G. Colangelo, M. Milanese and A. Risi (2015). Review of heat transfer in nanofluids: conductive, convective and radiative experimental results. *Renewable and Sustainable Energy Reviews* 43, 1182-1198.
- Mahaney, H. V., F. P. Incropera and S. Ramadhyani (1990). Comparison of predicted and measured mixed convection heat transfer from an array of discrete sources in a horizontal rectangular channel. *International Journal of Heat and Mass Transfer* 33(6), 1233-1245.
- Mahian, O., S. Mahmud and I. Pop (2012). Analysis of first and second laws of thermodynamics between two isothermal cylinders with relative rotation in the presence of MHD flow. *International Journal of Heat and Mass Transfer* 55(17), 4808-4816.
- Maxwel-Garnett, J. C. (1904). Colours in metal glasses and in metal films. *Philos. Trans. R. Soc. London* 203, 385-420.
- Mollamahdi, M., M. Abbaszadeh and G. A. Sheikhzadeh (2016). Flow field and heat transfer in a channel with a permeable wall filled with Al<sub>2</sub>O<sub>3</sub>-Cu/water micropolar hybrid nanofluid, effects of chemical reaction and

- magnetic field. *Journal of Heat and Mass Transfer Research (JHMTR)*.
- Nield, D. A. (2004). Forced convection in a parallel plate channel with asymmetric heating. *International Journal of Heat and Mass Transfer* 47(25), 5609-5612.
- Rahmati, A. R., A. R. Roknabadi and M. Abbaszadeh (2016). Numerical simulation of mixed convection heat transfer of nanofluid in a double lid-driven cavity using lattice Boltzmann method. *Alexandria Engineering Journal*.
- Raja, M., R. Vijayan, P. Dineshkumar and M. Venkatesan (2016). Review on nanofluids characterization, heat transfer characteristics and applications. *Renewable and Sustainable Energy Reviews* 64, 163-173.
- Sheikholeslami, M. and D. D. Ganji (2016). Nanofluid convective heat transfer using semi analytical and numerical approaches: A review. *Journal of the Taiwan Institute of Chemical Engineers*.
- Vanaki, S. M., P. Ganesan and H. A. Mohammed (2016). Numerical study of convective heat transfer of nanofluids: A review. *Renewable and Sustainable Energy Reviews* 54, 1212-1239.
- Vijayan, P. and C. Balaji (2004). Turbulent forced convection in a parallel plate channel with natural convection on the outside. *International communications in heat and mass transfer* 31(7), 1027-1036.
- Yao, L. S. (1983). Free and forced convection in the entry region of a heated vertical channel. *International Journal of Heat and Mass Transfer* 26(1), 65-72.